Salt inducible kinases control osteoblast maturation in alveolar bone

Salt inducible kinases control osteoblast maturation in alveolar bone

A Thesis Presented by

Nicha Tokavanich

to the Faculty of Medicine

In partial fulfillment of the requirements for the degree of

Doctor of Dental Medicine

Research Mentor: Marc Wein, MD, PhD, Associate Professor Harvard Medical School

Massachusetts General Hospital

Harvard School of Dental Medicine, Boston, Massachusetts

May 2024

Acknowledgments

I would like to express my deepest gratitude to Dr. Marc Wein, my thesis advisor, for his invaluable guidance, support, and patience throughout my DMSc journey. I am also extremely grateful to Dr. Wanida Ono for her helpful suggestions and support that enriched my learning experience. I express my appreciation to my thesis advisory committee and thesis defense committee, Dr. Francesca Gori, Dr. Yingzi Yang, Dr. Vicki Rosen, Dr. Henry Kronenberg, and Dr. Roland Baron for their insightful feedback.

Special thanks to Dr. Yuki Arai, Chris Castro, Katelyn Strauss, Dr. Noriaki Ono, and all members of the Wein laboratory and the Massachusetts General Hospital Endocrine Unit for their assistance in the research project and helpful discussions. I would also like to acknowledge the funding support provided by NIH and NIDCR.

To the faculty members and my co-residents of the Orthodontics department at Harvard School of Dental Medicine, your unwavering support and encouragement sustained me throughout my four-year journey.

Finally, I want to express my heartfelt gratitude to my beloved friends and family, especially my parents, my brother, and Top. Thank you for believing in me, supporting me in all my endeavors, and inspiring me to pursue my dreams.

Abstract

Alveolar bone serves to support and anchor teeth. It differs from most other skeletal tissue due to its unique origin from neural crest-derived mesenchymal cells and its formation through intramembranous ossification. The development of alveolar bone occurs coupled with tooth eruption through various signaling networks, including the parathyroid-related protein (PTHrP) pathway. Salt inducible kinases (SIKs) are important downstream regulators of PTH/PTHrP signaling in long bones, growth plate chondrocytes, and kidneys. Previous studies reported that the deletion of SIKs increases bone turnover and trabecular bone mass in long bones. However, the role of SIKs in alveolar bone remains unknown. To address this question, we used *Ubq-Cre*^{ERt2}*; Sik2*$^{f/f}$*; Sik3*$^{f/f}$ mice to perform tamoxifen-inducible global deletion in 3 different mouse models: development, adult onset, and following molar extraction. Tamoxifen-induced global deletion of SIK2/SIK3 was performed at postnatal day 3 in the developmental model, at postnatal week 12 in adult mice, and in some adult mice tooth extraction was performed 10 weeks post-tamoxifen injection. Surprisingly, compared to wild-type controls, SIK2/SIK3 mutant mice showed reduced alveolar bone mass in all models. Micro-CT demonstrated less bone volume and mineralization in the mutant alveolar bone lacking SIK2 and SIK3. Reduced alveolar bone in SIK2/SIK3 mutants was associated with reduced bone formation as assessed by calcein labeling. Furthermore, TRAP staining failed to show increased osteoclast activity, indicating that the alveolar bone loss is primarily caused by reduced bone formation rather than increased bone resorption. In regions of absent alveolar bone, increased alkaline phosphatase with reduced osteocalcin expression was noted, suggesting increased immature osteoblasts in the mutant mice lacking SIK2/SIK3. At 4 weeks post-tooth extraction, control maxillary first molar sockets displayed complete bone healing, while SIK2/SIK3 mutant mice exhibited absent bone healing in the tooth socket. The mutant extraction socket was filled with fibrous-like tissue showing increased alkaline phosphatase staining with decreased

osteocalcin expression, consistent with the developmental model result. Our results demonstrate that the absence of SIK2/SIK3 impairs terminal osteoblast maturation in alveolar bone. Taken together, these findings emphasize the importance of SIKs in alveolar bone osteoblast differentiation, maturation, and alveolar bone formation.

A. Background and Literature review

Alveolar bone

Alveolar bone is the bone that surrounds the teeth in the mandible and maxilla. It comprises two cortical plates separated by a spongy bone. Alveolar bone along with other periodontium, including periodontal ligament, cementum, and gingival tissue, are crucial for tooth support and mastication function. Similar to other skeletal tissue, alveolar bone functions as a reservoir for mineral and mesenchymal progenitor cells. However, unlike non-oral skeletal tissue, it originates from neural crest-derived dental follicular cells and primarily forms as a result of intramembranous ossification [1]. Alveolar bone formation requires the presence of dental follicle mesenchyme, suggesting that alveolar bone development depends on the presence of teeth[2]. Alveolar bone and the periodontium develop from intricate interactions between dental epithelium and ectomesenchyme during tooth eruption[3]. The remodeling and homeostasis of alveolar bone are influenced by the presence or absence of teeth and dystrophy, or injury of periodontium can result in tooth loosening or tooth loss, which can detrimentally affect a person's quality of life [4]. This complex structure is difficult to regenerate once it is lost, therefore, understanding the development, homeostasis, and healing of alveolar bone is critical for treating diseases and regenerating lost tissues. Alveolar bone biology is regulated by the interaction of many signaling pathways including the Hippo, Wnt/β-catenin, and Bone Morphogenetic Protein (BMP) signaling systems[5-10]. Calciotropic hormones such as parathyroid hormone and calcitonin, as well as other endocrine signaling effects from changes in hormone or inflammatory action can influence alveolar bone metabolism[11].

Parathyroid hormone and Parathyroid hormone-related protein pathway

The parathyroid hormone (PTH) and parathyroid hormone-related protein (PTHrP) pathway plays an essential role in proper tooth and bone development, mineral ion homeostasis, and bone turnover[12-17]. In craniofacial development, PTHrP signaling critically regulates tooth eruption and tooth root development. PTHrP-expressing dental follicular cells give rise to tooth root odontoblast, cementoblast, periodontal ligament cells, and alveolar bone[12,13]. It has been previously shown that autocrine signaling through the PTH/PTHrP receptor (PTH1R) maintains the physical cell fate of dental follicular mesenchymal cells to develop functional periodontium and induce normal tooth eruption. The lack of PTHrP signaling hampered tooth root formation, periodontal ligament formation, and tooth eruption. PTH1R deficiency causes cell fate shift of the PTHrP-positive mesenchymal progenitor cells away from normal periodontal cells into non-physiologic precocious cementoblast-like cells [13]. Loss-of-function PTH1R mutations result in primary failure of eruption in humans, a rare autosomal dominant disorder that is characterized by tooth eruption cessation despite an unobstructed eruption path with no other skeletal phenotype[18-20]. Many studies have shown that PTH and PTHrP play important roles in balancing bone production and bone resorption, with the effects varying depending on the quantity and frequency administered[7,21,22]. Anabolic effects of PTH include suppression of osteoblast apoptosis and enhanced terminal osteoblast differentiation [17,23]. Intermittent PTH administration stimulates bone formation and increases bone mass in both systemic and craniofacial bone[24].

Salt inducible kinases

Parathyroid hormone 1 receptor (PTH1R) is a G protein-coupled receptor (GPCR) that is activated by PTH and PTHrP[25]. Upon PTH1R activation, cAMP is upregulated along with other intracellular second messenger systems. Salt inducible kinases (SIKs) are a subfamily of AMP-activated protein kinase (AMPK) family kinases[26,27]. Previous studies have shown that SIKs are

important downstream targets of the PTH/PTHrP pathway in long bones. PTH/PTHrP signaling leads to PKA-dependent phosphorylation and inactivation of SIKs. Once SIK activity is inhibited, phosphorylation levels of SIK substrates such as class IIa HDAC and CRTC proteins are decreased, resulting in nuclear translocation and target gene regulation. Nuclear class IIa HDACs primarily restrict MEF2-driven gene expression, whereas nuclear CRTC proteins coactivate CREB-regulated target genes[26-29]. In osteocytes in bone, the Mef2 family transcription factor controls sclerostin expression and the CREB-related target gene induces RANKL gene expression. HDAC4/HDAC5 are essential for PTH to inactivate sclerostin which increases bone formation, while CRTCs are crucial for RANKL upregulation, which increases bone resorption[30,31]. Combined deletion of SIK2 and SIK3 globally and specifically in osteoblast and osteocyte resulted in dramatic increased trabecular bone mass, and increased bone turnover, while the thickness of cortical bone is decreased along with increased its porosity[26,31].

Other possible related pathways

Wnt/ β-catenin signaling pathway

The Wnt/ β-catenin signaling pathway plays an important role in embryonic development and adult tissue homeostasis. The canonical Wnt pathway regulates cellular function by modulating intracellular levels of β-catenin through interactions with Frizzled (FZD) receptors. When activated, the Wnt pathway stabilizes β-catenin and transports it to the nucleus, promoting target gene expression[39]. Upon the absence of Wnt ligand, β-catenin binds to a protein complex containing adenomatous polyposis coli (APC), Axin, and Glycogen synthase kinase 3 (GSK3), then targeted for degradation[40]. Wnt signaling operates with the BMPs and Hedgehog pathways, both of which control bone development and formation. Additionally, Wnt/β-catenin signaling influences the fate of mesenchymal progenitor cell differentiation, favoring osteogenic lineage over chondrocyte or adipocyte differentiation.[41-44]. There may be a

role of Wnt signaling in alveolar bone homeostasis and healing. Sclerostin and DKK1, Wnt signaling inhibitors, have been identified as crucial factors contributing to alveolar bone loss during the progression of periodontitis[45]. Furthermore, activation of Wnt signaling facilitates alveolar bone healing in an inflammatory environment, such as periodontitis[46].

Study Aims

In long bone, combined SIK2 and SIK3 deletion (either globally or selectively in osteoblasts/osteocytes) leads to dramatic increases in trabecular bone mass but reduced cortical bone with cortical porosity[47]. To date, the role of these kinases in tooth and jawbone development and homeostasis remains unknown. Based on their role in long bone PTH/PTHrP actions, we hypothesize that SIKs function as downstream targets of PTH/PTHrP pathway in alveolar bone. Consequently, we propose that the genetic deletion of SIKs will result in constitutive activation of PTH/PTHrP signaling, resulting in accelerated tooth eruption[48]. To test our hypothesis, we pursued three specific aims: (1) To assess the role of salt-inducible kinases in alveolar bone development. (2) To assess Salt-inducible kinases' role in alveolar bone homeostasis. (3) To assess Salt-inducible kinases' role in alveolar bone healing.

C. Research Design and Methods

Study samples.

Genetically modified mice

All animals were housed in the Center of Comparative Medicine at the Massachusetts General Hospital and all experiments were approved by the hospital's Subcommittee on Research Animal Care. The following published genetically modified strains were used: SIK2 floxed mice (RRID: MGI: 5905012), *SIK2*$^{tm1a(EUCOMM)Hmgu}$ mice (RRID: MGI 5085429) were purchased from EUCOMM and bred to PGK1-FLPo mice (JAX #011065) in order to generate mice bearing a loxP-flanked SIK3 allele[31]. *Ubiquitin-Cre*^{ERt2} mice[49] (JAX #008085). Cre^{ERt2}-negative littermate controls were used for all studies to account for the potential influence of

genetic background and the impact of tamoxifen on bone development and homeostasis. All mice were backcrossed to C57B1/6J for at least five generations.

Tamoxifen (Sigma-Aldrich, St. Louis, MO catalog #T5648) was dissolved in absolute ethanol. Sunflower oil (Sigma, catalog #99021-250 ML-F) is added in equal amounts at concentrations of 5 or 20 mg/mL. To develop specific mouse models, Tamoxifen was administered to induce global deletion of SIK2/SIK3 at different time points. Three mouse models were generated for each specific aim:

Specific Aim I: Developmental model

We examined control (*Sik2$^{f/f}$;Sik3$^{f/f}$*) and double mutant mice (*Ubiquitin-Cre^{ERt2}*; *Sik2$^{f/f}$;Sik3$^{f/f}$*) [32]. All mice were treated with 0.25 mg of tamoxifen at postnatal day 3. Then, mice were sacrificed at postnatal days 8, 11, 14, 21, and 28. Histology, micro-CT, and histomorphometry of the mandible was examined.

Specific Aim II: Adult model

We studied control (*Sik2$^{f/f}$;Sik3$^{f/f}$*) and double mutant (*Ubq-Cre^{ERt2}*; *Sik2$^{f/f}$;Sik3$^{f/f}$*) mice. All mice were treated with 1mg/kg of tamoxifen 3 times every other day for a week at 12 weeks of age, then sacrificed at 2 weeks, 8 weeks, and 10 weeks post-injection. The histology and micro-CT of the mandibles were examined at the cellular and tissue mineralization levels.

Specific Aim III: Tooth extraction model

We studied control (*Sik2$^{f/f}$;Sik3$^{f/f}$*) and double mutant (*Ubq-Cre^{ERt2}*; *Sik2$^{f/f}$;Sik3$^{f/f}$*) mice. All mice were treated with tamoxifen at 12 weeks of age. We waited for 10 weeks to allow gene deletion and its consequences on alveolar bone biology. For each surgical procedure, mice were pre-anesthetized in an induction chamber with 3-4% Isoflurane and oxygen through an isoflurane vaporizer until the animal was in lateral recumbency. The mouse was then placed on the surgery operating area in a nose cone that provides appropriate doses of isoflurane and oxygen to maintain a surgical plane of anesthesia. The first maxillary molars on both sides were extracted under general anesthesia using dental extraction forceps for rodents. These mice

were sacrificed 4 weeks after the extraction, then maxillae were collected and fixed in 4% PFA overnight for micro-CT scanning and histology sections.

Histology

Mouse mandibles and maxillae were carefully dissected and fixed in 4% Paraformaldehyde (pH 7) overnight at 4 degrees Celsius. Both jaws were then decalcified in 15% EDTA for 1-14 days. After decalcification, samples were cryoprotected in 30% sucrose/PBS overnight followed by 1:1 30% sucrose/PBS: optimal cutting temperature (OCT) compound solution overnight. Samples were embedded in OCT compound and cryo-sectioned at 12 µm thickness. H&E and DAPI staining were performed on some sections using standard protocols.

TRAP staining

TRAP staining was performed to identify osteoclasts. Sections were immersed in acetate buffer (pH 5.0 at room temperature) for 30 minutes. Napthol AS-MX Phosphate and Fast Red TR Salt were added to the solution, then the sections were incubated in TRAP staining solution at 60 degrees Celsius for 10-20 minutes. Lastly, sections were counter-stained with Fast Green solution.

Fluorochrome labeling

To evaluate bone deposition, developmental model mice were given Calcein (20mg/kg) intraperitoneal injection on postnatal days 10 and 12, and sacrifice mice at P14. Mandibles were dissected, fixed in 4% Paraformaldehyde overnight, then cryoprotected with 30% sucrose/PBS overnight, and 1:1 30% sucrose/PBS: OCT overnight. Uncalcified samples were embedded in OCT compound and cryo-sectioned at 12 µm.

Von Kossa staining

To distinguish the mineralized bone matrix from the non-mineralized bone matrix, Von Kossa staining was performed. P14 uncalcified sections were incubated in 1% Silver Nitrate under a 60-watt UV lamp for 25 minutes, then 2% sodium thiosulphate for 2 minutes to stop the reaction, and lastly, sections were counterstained with Fast Green.

Alkaline phosphatase staining

To check for immature osteoblast activity, alkaline phosphatase staining was performed. Sections were immersed in Tris Buffer (pH 9.4) at room temperature for 1 hour, then incubated in alkaline phosphatase staining solution (Tris buffer pH 9.4, Fast Blue solution, Napthol ASBI Phosphate solution, and Magnesium chloride) at 37 degrees Celsius for 10-20 minutes.

Immunohistochemistry

Anti-periostin and anti-osteocalcin immunofluorescent staining

Sections were postfixed with 4% PFA for 20 minutes. Then sections were permeabilized with 0.1% Triton-X/TBS for 30 minutes, blocked with 5% BSA/TBST for 30 minutes, and then incubated with primary antibody at 4 degrees Celsius overnight with anti-Periostin rabbit antibody (1:2000, ABT280 Sigma-Aldrich), or anti-Osteocalcin rabbit antibody (1:200, AB93876 Abcam). After overnight incubation, sections were immersed in secondary antibody conjugated with AlexaFlour 488 (A21206), or 568 (A10042) at 4 degrees Celsius overnight. Lastly, the counterstaining was done using DAPI before imaging.

Three-dimensional micro-computed tomography analysis of mouse samples.

The assessment of alveolar bone morphology and architecture was performed using micro-CT analysis. After fixation with 4% PFA, both mandible and maxilla were kept in PBS and scanned as DICOM file on a micro-CT system (μCT40; Scanco Medical, Brüttisellen,

Switzerland) using 70 kVp peak X-ray tube potential, 113 mAs X-ray tube current, 200 ms integration time, and 10 μm isotropic voxel size. To quantify the distance between anatomical points, three-dimensional volumetric label maps, also called segmentation, were generated from DICOM files using ITK-SNAP open software. The segmentation of each sample was created with each molar labeled separately and converted to a 3D surface model in Slicer open-source software. Measurements were done with Q3DC tool in Slicer open-source software as previously published study[33].

To quantify the mineralization tissue in alveolar bone, the interradicular bone of the first molars was chosen as an area of interest in development and adult mice. For the tooth extraction model, the mesial root of the maxillary first molar socket was chosen as an area of interest. We measured alveolar bone volume fraction (BV/TV, %) and alveolar bone mineral density (BMD). Bone was segmented from soft tissue using a fixed threshold of 550 mg HA/cm3. The scanning and analyses followed the guidelines for using micro-CT to examine bone architecture in rats. The micro-CT analysis was performed on a blinded basis with all animals assigned coded sample numbers[50].

Statistical analysis

Variables from micro-CT measurement, including tooth root length, crown with and height, interradicular bone height, tooth eruption, bone volume fraction (BV/TV, %), and alveolar bone mineral density (BMD) were collected. Unpaired T-test was performed to compare means of each variable between control and mutant samples. A p value of less than 0.05 was considered to be statistically significant.

D. Results

SIK2 and SIK3 are crucial for alveolar bone development.

We first used genetic models to study the role of Salt-inducible kinases in alveolar bone development. Of the three mammalian SIK isoforms, SIK2 and SIK3 (genes that are closely linked on syntenic regions of mouse chromosome 9 and human chromosome 11) play critical roles downstream of PTH1R action in bone and kidney[29,47,51]. Therefore, first, we used *Sik2$^{f/f}$; Sik3$^{f/f}$;* and *ubiquitin-Cre^{ERt2}* (mutant) mice to ubiquitously delete SIK2 and SIK3. Mutant and control (*Sik2$^{f/f}$; Sik3$^{f/f}$)* mice were treated with tamoxifen at P3 to induce the inhibition at the time of first mandibular molars eruption, to induce the deletion. Mandibles were then analyzed at P8, P11, P14, P21 and P28. At P8, no difference was found between mutant and control mandible. Unexpectedly, starting at P11, reduced alveolar bone in SIK2/SIK3 mutants was observed. By P21, a complete lack of alveolar bone was noted in SIK2/SIK3 mutant mandibles in both inter-radicular and inter-septal bone regions. The mutant alveolar bone was replaced with fibrous-like tissue **(Figure 1).**

Von Kossa staining was performed to better illustrate the mineralization tissue of the alveolar bone area at P14. Less mineralization tissue was noticed in the mutant mandible. Analysis of long bones at P28 from mice injected with tamoxifen at P3 revealed expected changes due to SIK2/SIK3 ablation including expansion of proliferating chondrocytes[52] and increased trabecular bone[31] **(Figure 4)**.

Micro-CT analysis was performed on P28 mandibles to quantify the effects of global SIK2/SIK3 deletion in alveolar bone and tooth eruption. Morphologically, mutant mandibles were smaller compared to control. The mutant mandibles were expanded in the sagittal plane with increased porosity of cortical bone. The most evident phenotype seen in SIK mutant mandibles was a punched-out lesion around molars which confirms the absence of alveolar bone in H&E and Von Kossa staining. Bone volume fraction in this region was reduced to almost zero in the mutant mandible **(Figure 2)**. In sum, our histology and micro-CT analysis of jaws at P28 following SIK2/SIK3 ablation at P3 revealed an unexpected and dramatic loss of alveolar bone.

Remarkably, despite the lack of alveolar bone, tooth eruption occurred normally in SIK2/SIK3 mutant mandibles.

Our next question was whether the observed alveolar bone defects were due to decreased bone formation or increased bone resorption. First, we performed TRAP (tartrate-resistant acid phosphatase) staining to evaluate osteoclast number since the deletion of SIK2/SIK3 increases RANKL expression and osteoclast activity in long bones[47]. Surprisingly, no significant difference in TRAP staining was found in P8 and P11 mandibles. However, starting from P14, reduced TRAP staining was noted in the alveolar bone area of mutant mandibles. Our data consistently revealed no elevation in TRAP staining across all time points **(Figure 3)**. This suggested that increased bone resorption does not contribute to this lack of alveolar phenotype. Next, we checked the bone deposition with fluorochrome labeling. We observed significantly decreased Calcein deposition in the alveolar bone area in SIK2/SIK3 mutants compared to controls **(Figure 4).** Taken together, these results suggested that defective alveolar bone formation, rather than increased bone resorption, was mainly responsible for reduced alveolar bone mass in SIK2/SIK3 mutants.

In long bones, SIK2/SIK3 deletion with *ubiquitin*-Cre^{ERt2} causes dramatic increases in trabecular bone mass due to increased bone formation.[31] Therefore, *reduced* alveolar bone formation in this same model was unexpected. To explore this unexpected observation, we performed alkaline phosphatase and osteocalcin (Ocn) staining (markers of early and mature osteoblasts, respectively) to evaluate osteoblast maturation in control and mutant alveolar bone regions at P28. Despite observing reduced in mineralized tissue and calcein deposition, we noted increased alkaline phosphatase expression in mutant mandibles. However, these alkaline phosphatase-positive cells failed to upregulate osteocalcin, suggesting that SIK2/SIK3 deficiency impedes the final stages of alveolar bone osteoblast maturation **(Figure 5)**. Taken

together, these results demonstrate that SIK2 and SIK3 play important roles in alveolar bone osteoblast maturation.

PTH1R deletion in PTHrP-positive dental follicular cells resulted in failure of tooth eruption and impaired PDL differentiation, causing a shift in cell fate from PDL and acellular cementum to cementoblast-like cells [12]. Since PTH1R signaling inhibits cellular SIK2/SIK3 activity, we wondered if SIK2/SIK3 deletion might lead to a phenotype opposite that of PTH1R deficiency, or a phenotype like what is observed with constitutively active PTH/PTHrP signaling in the jaw. Notably, decreased Periostin (POSTN, a marker of PDL fibroblast[53]) levels were noted in the PTH1R deficiency model[13]. Therefore, we performed POSTN immuno-staining at all time points. At P8-P14, no significant differences were found between wild-type and mutant mandibles. At P21 and P28, increased POSTN-positive cells were noted in double knockout inter-septal and inter-radicular areas in regions of absent mineralized tissue **(Figure 6).** This finding suggests that the lack of SIK2 and SIK3 affects mesenchymal cell differentiation and shifts the cell population from mature bone-forming osteoblasts to ectopic POSTN-positive cells.

SIK2 and SIK3 have important roles in alveolar bone maintenance in adult mice.

Until now, genetic studies have ablated SIKs during early postnatal development (P3 tamoxifen injection). As such, the role of SIKs in alveolar bone homeostasis remains unknown. Therefore, we ubiquitously deleted SIK2/SIK3 in 12-week-old mice to examine the role of SIKs in alveolar bone homeostasis in skeletally-mature mice. At 12 weeks of age, we injected tamoxifen and collected mandibles after 2, 8, and 10 weeks later. At 2 weeks post-injection, no major phenotypic differences were noted between control and mutant littermates. However, at 8 and 10 weeks after tamoxifen-induced SIK2/SIK3 deletion, alveolar bone loss was seen in mutant mice in both interradicular and interseptal areas **(Figure 7)**.

We performed micro-CT analysis in mandibles obtained 10 weeks after adult-onset SIK2/SIK3 deletion to further investigate changes in mature alveolar bone. There was no significant difference in the size of the mandibles. However, in contrast to the global SIK2/3 deletion long bone phenotype[47], decreased alveolar bone density was observed in the knockout mice. BV/TV of mutant alveolar bone also slightly reduced and bone mineral density was significantly reduced, indicating that SIK2/SIK3 deletion affects both alveolar bone formation and maintenance **(Figure 8)**.

TRAP staining in the alveolar bone area of the mutant mandible was reduced at P8 and 10 weeks post-injection. Our result showed no elevation of TRAP-positive cells, consistent with the phenotype observed in the developmental model. As a result, alveolar bone loss is most likely caused by decreased bone production rather than increased bone resorption **(Figure 9)**. These findings indicate the significance of SIK2 and SIK3 in maintaining optimal alveolar bone health, as they play an important role in regulating the intricate balance between bone formation and resorption throughout homeostasis.

SIK2 and SIK3 are crucial for tooth socket healing in adult mice.

Healing of the alveolar bone after tooth extraction is a major research focus, as alterations in the alveolar bone can profoundly impact the aesthetic and stability outcomes of dental prosthetic procedures at a later stage. However, the role of SIKs in alveolar bone healing remains unexplored. We induced ubiquitous SIK2/SIK3 deletion in 12-week-old mice, then extracted the first maxillary molars 10 weeks later. At 4 weeks post-extraction, the control maxillary socket demonstrated complete bone healing, as evidenced by the presence of organized epithelium and mineralized bone within the extraction socket. In contrast, SIK2/SIK3 mutant sockets exhibited an absence of bone formation with tooth sockets instead filled with fibrous-like tissue. Micro-CT confirmed absent mineralization within the healed extraction sockets in the SIK2/SIK3 mutant maxilla **(Figure 10)**.

To assess osteoblast activity in this model, alkaline phosphatase and Ocn immuno-staining were performed. In mutant mice, elevated alkaline phosphatase staining throughout the tooth socket was noted. Conversely, reduced osteocalcin expression was detected at the socket floor in mutant mice, aligning with findings in the developmental model. We then used Periostin immuno-staining to identify the fibrous-like tissue that replaces the bone during tooth socket healing—these POSTN-positive fibrous tissues indicate PDL expansion in mutant mice **(Figure 11)**. Our findings indicate that SIK2 and SIK3 are essential in promoting successful tooth socket healing. Specifically, they control osteoblast maturation and may influence cell fate shifting of mesenchymal progenitor cells toward the osteogenic pathway, contributing to a complex process of tissue regeneration in the extraction socket.

In sum, these results indicate that SIK2/SIK3 plays crucial roles in optimal alveolar bone formation in development, adult homeostasis, and in the setting of tooth extraction healing due to a key role in alveolar bone osteoblast maturation.

E. Discussion

Our findings indicate that SIK2/SIK3 are essential for normal alveolar bone development and alveolar bone homeostasis/remodeling. Alveolar bone defects in SIK2/SIK3 mutant mice are associated with severe socket healing following molar extraction. Reduced alveolar bone mineralization was found in alveolar bone in mutant mandible and maxilla. Decreased osteoclast activity was found in all models, suggesting that alveolar bone defect is primarily caused by decreased bone formation rather than increased bone resorption. Unexpectedly, we observed a significant increase in alkaline phosphatase expression without upregulation of the osteoblast maturation marker osteocalcin in both developmental and tooth extraction models. The alveolar bone region of developmental mutant mice is replaced with fibrous-like tissue. This tissue displayed positive POSTN staining, suggesting periodontal ligament replacement within

the expected alveolar bone location. This observed finding may be attributed to the absence of SIK2/SIK3, resulting in a shift in cell fate from skeletal lineage cells to periodontal ligament lineage cells.

The phenotype we observe in SIK2/SIK3 mutant mice shares some resemblance to hyperparathyroidism, which is known to cause alveolar bone loss. Previous research has shown that patients with hyperparathyroidism have reduced alveolar bone density and are more likely to show extension of the periodontal ligament space around their teeth. Notably, the degree of this enlargement corresponds with the degree of PTH elevation in blood[54]. Furthermore, hyperparathyroidism is associated with decreased cortical bone density in mandibular bone[55]. However, previous studies have reported that bone defects typically associated with hyperparathyroidism are primarily attributed to increased bone resorption, in contrast to our findings which suggest that reduced bone formation by mature alveolar bone osteoblasts is the primary defect in the absence of SIK2/SIK3. Mandible with global SIK2/SIK3 deletion share similarities with Fibrous Dysplasia (FD), with abnormal fibro-osseous tissue replacing regular bone. The FD etiology is mutations of the GNAS gene, resulting in overproduction of cAMP and over-activation of Wnt/β-catenin signaling pathway. Whether increased protein kinase A signaling in FD leads to SIK inhibition remains unknown. FD-derived osteoblasts produce higher PTHrP compared to cells derived from healthy control patients[56,57]. PTHrP can modulate both cAMP/PKA/CREB and Canonical Wnt/b-Catenin signaling pathways, influencing osteogenic differentiation and proliferation in BMSCs. This suggests that there may be a potential involvement of the Wnt/Beta-catenin pathway and PTH signaling pathway in the development of alveolar bone defects with decreased osteogenesis[56]. At present, further study is needed to unravel the molecular mechanism whereby SIK2/SIK3 controls osteoblast maturation selectively in the alveolar bone.

One major limitation of our study lies in the fact that we globally eliminated SIKs in all tissues using the broadly-expressed ubiquitin-Cre^{ERt2} driver. This approach makes it challenging to pinpoint the precise cell type in which SIK2/SIK3 gene deletion causes alveolar bone defects. For example, it remains possible that systemic mineral metabolism parameters, such as hypercalcemia or high 1,25-vitamin D levels, seen in global SIK2/SIK3 mutants might indirectly affect alveolar bone development and remodeling[51]. Therefore, while our study provides valuable insights into the importance of SIKs in alveolar bone, it cannot definitively establish a direct alveolar bone-autonomous function of SIKs. Future studies with inducible cell type-specific SIK2/SIK3 deletion should shed further light on this important topic. Another limitation of our study is that we performed tooth extractions after 10 weeks of SIK2/SIK3 deletion, by which time alveolar bone defects had already occurred prior to the extractions. While we can infer that SIK2/SIK3 is essential for alveolar bone healing following tooth extraction, it is important to acknowledge that the absence of alveolar bone from the outset may exacerbate the bone healing challenges observed in our extraction model. A new study design has been planned to address this limitation. This design involves injecting tamoxifen 12 weeks after birth, followed by tooth extraction two weeks later. The purpose of this timeframe is to ensure complete gene deletion without causing any alveolar bone loss before the extraction procedure. This will allow us to determine the effect of SIK2/SIK3 deletion on tooth socket healing without compromised alveolar bone during the tooth extraction. On the other hand, the adult-onset SIK2/SIK3 mutant mice with absent alveolar bone could provide an excellent model to assess the relationship between intact alveolar bone tissue and subsequent healing following molar extraction.

Furthermore, our study discovered that, despite the absence of alveolar bone in SIK2/SIK3 global/inducible mutant mice, both tooth eruption and root formation remain unaffected. This finding highlights our limited understanding of the intricate interplay between tooth eruption and its underlying alveolar bone and suggests that tooth eruption and alveolar bone formation may not be mutually dependent processes.

Our study revealed a striking divergence in the observed phenotypes between long bones and alveolar bone in response to SIK2/SIK3 deletion. While global deletion of SIK2/SIK3 in long bones results in increased trabecular bone mass, increased bone formation, and increased bone turnover[47], bone defects with decreased bone formation can be noted in alveolar bone. This highlights the fact that different bones within the body exhibit unique behavior and responses to SIK2/SIK3 deletion. This divergence could be attributed to different cell origins and developmental mechanisms between these bone types. Long bone derives from mesenchymal cells through endochondral ossification[58], whereas alveolar bone forms from ectomesenchymal neural crest cells through intramembranous ossification[1]. Additionally, the unique oral microenvironment, mechanical forces, and local signaling factors may further underlie the different behaviors. Our study emphasizes the need to consider the unique properties and origins of different bones while studying their development and reactions to genetic changes.

F. Ongoing/Future directions

To address the study's limitations, we induced SIK2/SIK3 deletion using the *Osx*-Cre^{ERt2} strain, allowing inducible deletion in mesenchymal/osteogenic lineage cells[12]. Tamoxifen injection in control (*Osx*-Cre^{ERt2}; Tm/Tm) and mutant (Osx-Cre^{ERt2}; *Sik2*$^{f/f}$; *Sik3*$^{f/f}$; Tm/Tm) mice was performed at P3, and animals were then sacrificed at P28. Sagittal expansion of mutant mandibles was found. H&E staining showed reduced alveolar bone in the mutant mandible, albeit to a lesser degree than what was observed in *Ubq*-Cre^{ERt2}*; Sik2*$^{f/f}$*; Sik3*$^{f/f}$ animals. Micro-CT demonstrated a trend of less bone volume and significantly less bone mineral density in the alveolar bone region. TRAP staining was increased in *Osx*-Cre^{ERt2} SIK2/SIK3 mutant mice, indicating (in contrast to our global/inducible SIK2/SIK3 deletion model) increased bone resorption in this mouse model. We are currently collecting additional samples and investigating the molecular changes occurring in these knockout mice.

To elucidate the specific pathways influenced by SIKs deletion in alveolar bone, next we will utilize single-cell RNA sequencing to compare different gene expression levels between SIK-deleted alveolar bone cells versus and control samples.

Our findings demonstrate that there are notable distinctions between alveolar bone and long bone with respect to the consequences of SIK2/SIK3 gene ablation. To gain insights into different gene regulatory programs that might underlie this distinct phenotype between osteoblasts of different anatomic origin, we will compare available single-cell RNA profiles between long and alveolar bone osteoblasts. This can uncover unique signatures that underlying biological mechanisms governing their distinct function and responses to various stimuli and offer crucial insights for both basic bone biology and clinical application in dentistry and orthopedics.

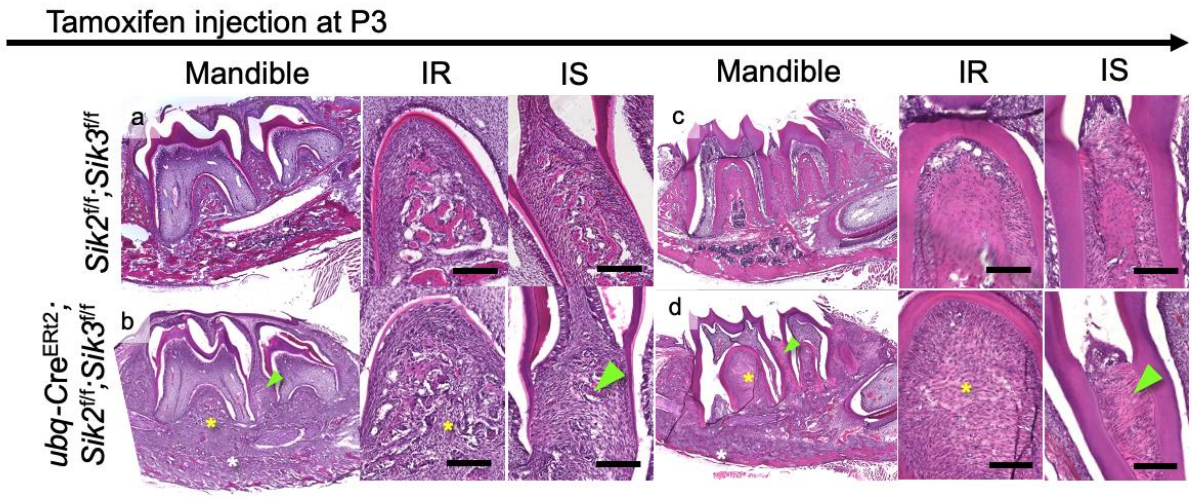

Figure 1: Alveolar bone defects found in mutant mice starting at P14

a, b: H&E staining of control and globally SIK2/SIK3 deleted mandible at P14

c, d: H&E staining of control and globally SIK2/SIK3 deleted mandible at P28

Green arrowhead: Bone defects in interseptal area, Yellow asterisk: Bone defects in interradicular area, IR = Interradicular bone area, IS = Interseptal bone area.

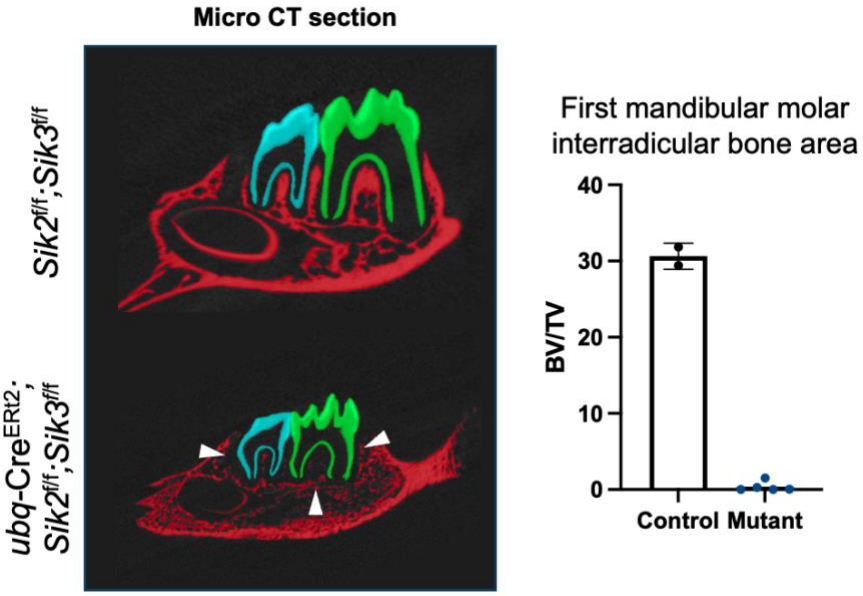

Figure 2: Micro-CT data showed less Bone volume fraction in the mutant alveolar bone at P28

Red: Alveolar bone, Green: Mandibular first molar, Blue: Mandibular second molar

White asterisk: Alveolar bone defect in mutant mandible

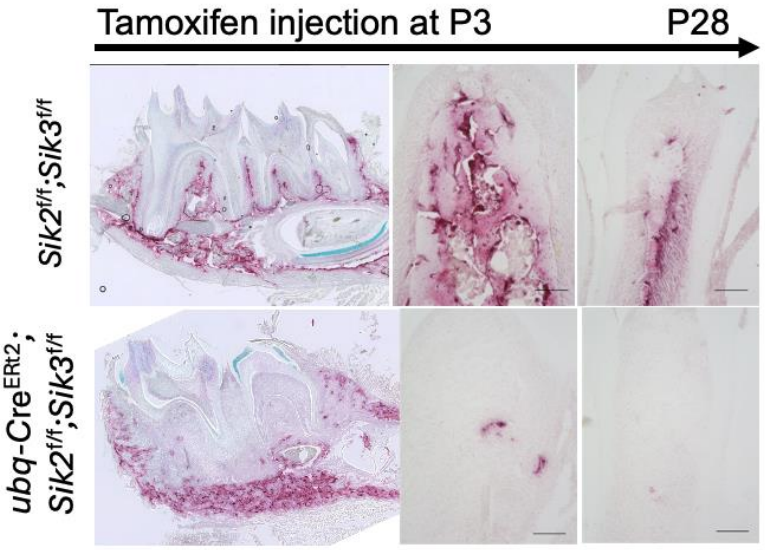

Figure 3: Reduced TRAP staining in P28 alveolar bone

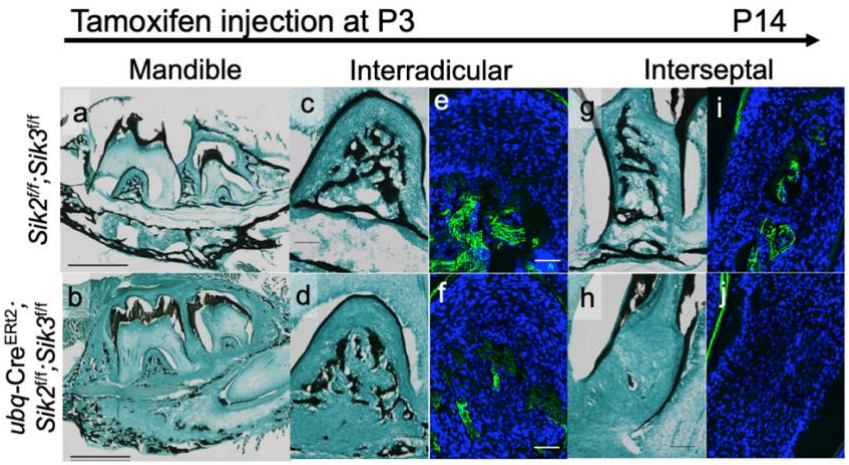

Figure 4: Less bone deposition with less mineralized tissue in mutant alveolar bone at P14

a,b: Von Kossa staining of control and mutant mandible at P14

c,d: Von Kossa staining of control and mutant mandibular first molar interradicular bone

e,f: Calcein labeling of control and mutant mandibular first molar interradicular bone

f,h: Von Kossa staining of control and mutant mandibular first molar interseptal bone

i,j: Calcein labeling of control and mutant mandibular first molar interseptal bone

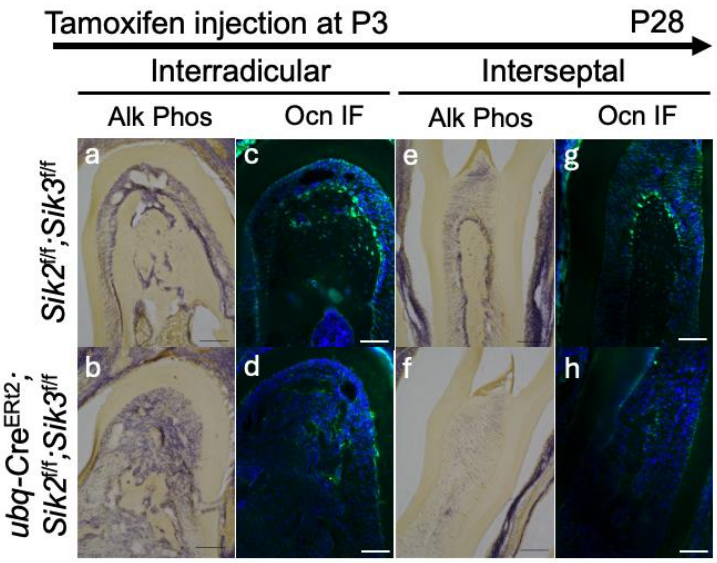

Figure 5: Increased immature osteoblast, while decreased mature osteoblast found in mutant alveolar bone

a,b: Alkaline phosphatase staining of control and mutant mandibular first molar interradicular bone at P28

c,d: Anti-Osteocalcin immunofluorescent staining of control and mutant mandibular first molar interradicular bone at P28

e,f: Alkaline phosphatase staining of control and mutant mandibular first molar interseptal bone at P28

g,h: Anti-Osteocalcin immunofluorescent staining of control and mutant mandibular first molar interseptal bone at P28

Purple: Alkaline phosphatase staining, Green: Anti-Osteocalcin immunofluorescent, Blue: DAPI staining

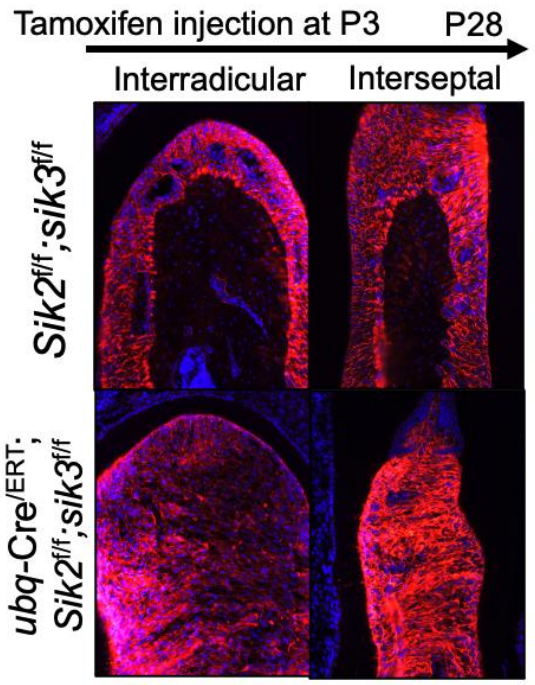

Figure 6: Periostin-positive fibrous tissue replaced alveolar bone in mutant mandible.

Red: Anti-Periostin immunofluorescent, Blue: DAPI staining

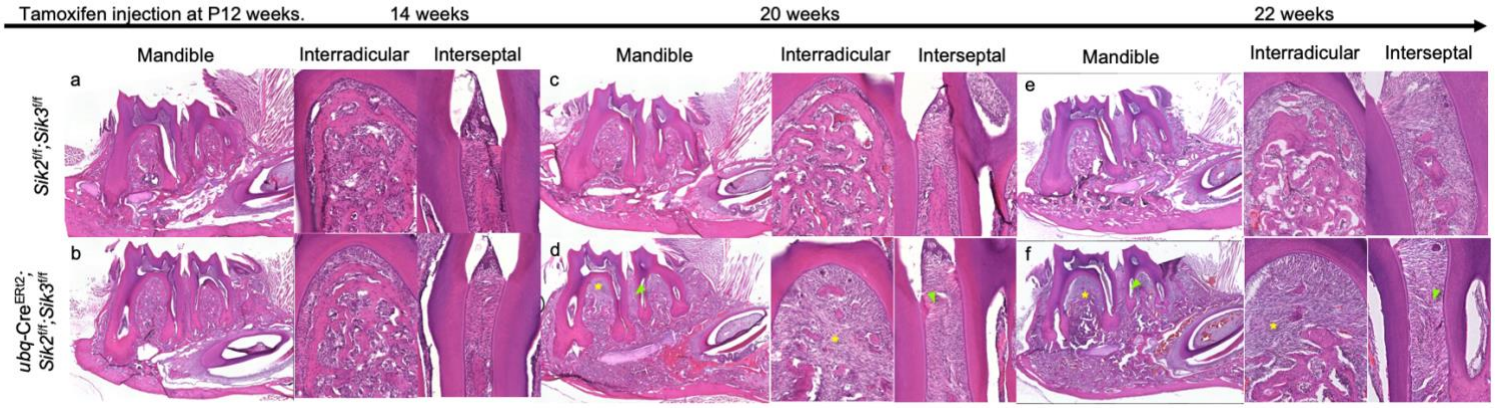

Figure 7: Alveolar bone defects found in adult mutant mandible starting at 8 weeks after Tamoxifen injection.

a,b: H&E staining of mandible, interradicular bone, and interseptal bone of control and mutant mice 2 weeks after Tamoxifen injection.

c,d: H&E staining of mandible, interradicular bone, and interseptal bone of control and mutant mice 8 weeks after Tamoxifen injection.

e,f: H&E staining of mandible, interradicular bone, and interseptal bone of control and mutant mice 10 weeks after Tamoxifen injection

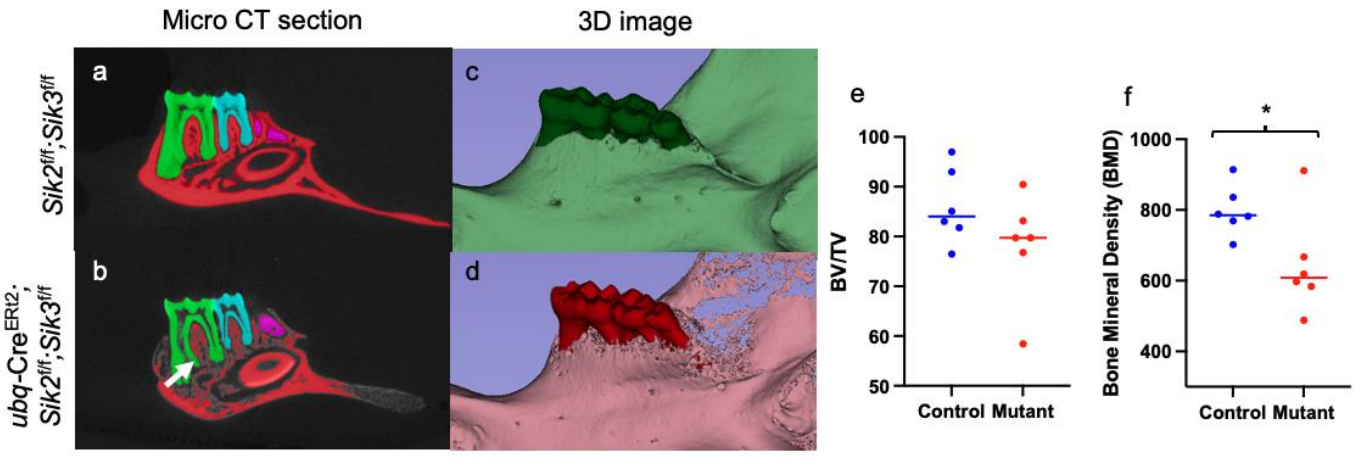

Figure 8: Micro CT data showed less bone volume fraction and bone mineral density in mutant alveolar bone at 10 weeks after Tamoxifen injection.

a,b: Micro CT sections of control and mutant mandible.

Red: Alveolar bone, Green: Mandibular first molar, Blue: Mandibular second molar, Purple: Mandibular third molar

c,d: Three-dimensional images of control and mutant alveolar bone and teeth.

Green: Control teeth and mandible, Red: Mutant teeth and mandible

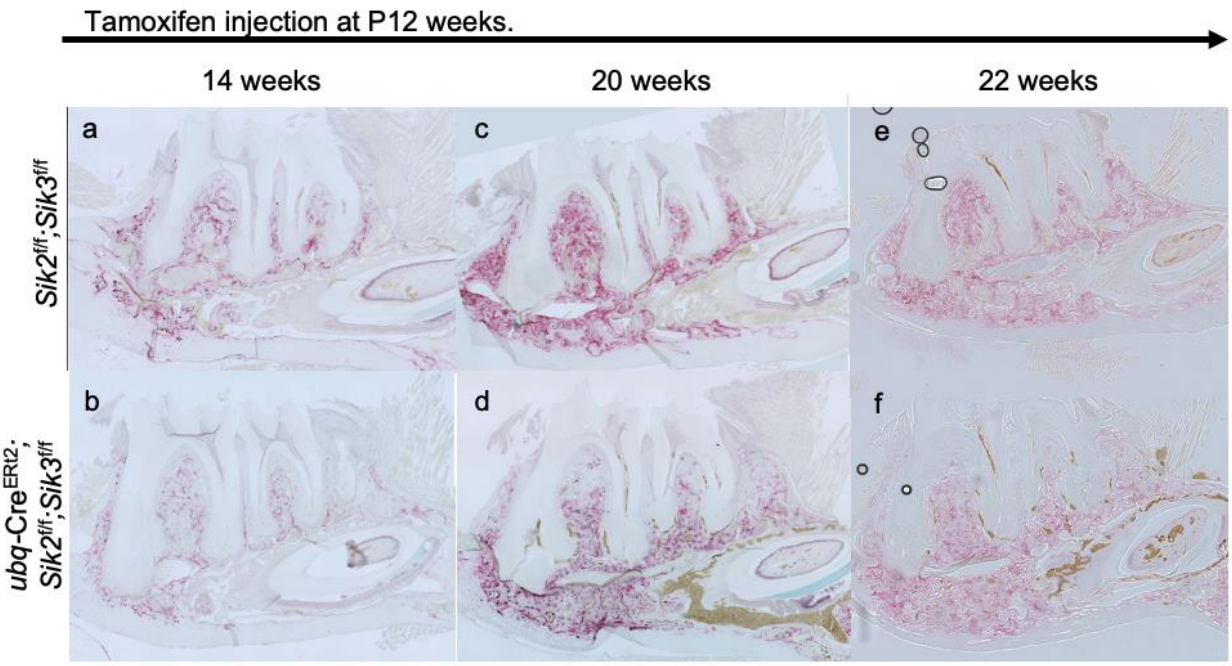

Figure 9: Less TRAP staining in mutant alveolar bone at 8 and 10 weeks after Tamoxifen injection

a,b: TRAP staining of control and mutant mandibles at 2 weeks after Tamoxifen injection

c,d: TRAP staining of control and mutant mandibles at 8 weeks after Tamoxifen injection

e,f: TRAP staining of control and mutant mandibles at 10 weeks after Tamoxifen injection.

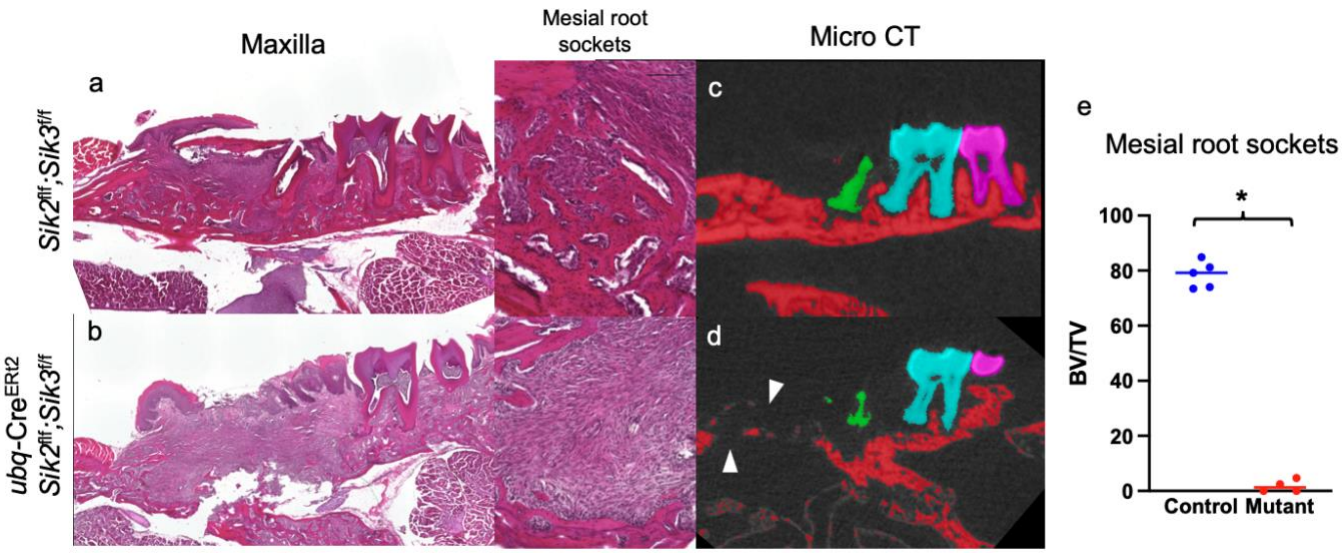

Figure 10: Impaired tooth socket healing found in mutant maxilla 4 week after tooth extraction.

a: H&E staining of control maxilla and mesial root socket.

b: H&E staining of mutant maxilla and mesial root socket.

c: Micro CT section of control maxilla

d: Micro CT section of mutant maxilla

Red: Alveolar bone, Green: Maxillary first molar root, Blue: Maxillary second molar, Purple: Maxillary third molar, White arrowheads: Impaired tooth socket

e: Bone volume fraction of control and mutant mesial root sockets.

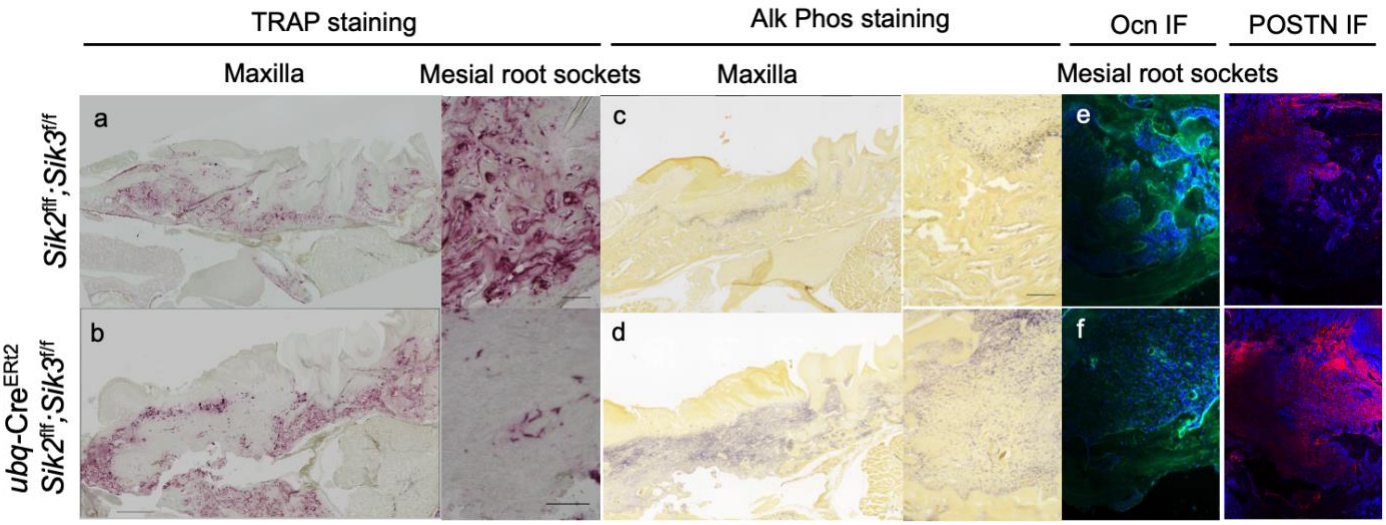

Figure 11: Less TRAP staining, increased Alkaline Phosphatase, and decreased Osteocalcin expression in mutant tooth extraction sockets.

a,b: TRAP staining of control and mutant maxillary first molar tooth extraction sockets.

c,d: Alkaline Phosphatase staining of control and mutant maxillary first molar tooth extraction sockets.

e,f: Anti-Osteocalcin immunofluorescent of control and mutant maxillary first molar tooth extraction sockets.

g,h: Anti-Periostin immunofluorescent of control and mutant maxillary first molar tooth extraction sockets.

F. Reference

1. Nanci A. Nanci A, ed. *Ten Cate's Oral Histology*. 9th ed. Elsevier; 2017.

2. Hall BK. *Bones and Cartilage*. Chapter 25 - Diversity of Bone as a Tissue and as an Organ. Academic Press; 2015.

3. Lumsden AG. Spatial organization of the epithelium and the role of neural crest cells in the initiation of the mammalian tooth germ. *Development*. 1988;103 Suppl:155-69. doi:10.1242/dev.103.Supplement.155

4. Pagni G, Pellegrini G, Giannobile WV, Rasperini G. Postextraction alveolar ridge preservation: biological basis and treatments. *Int J Dent*. 2012;2012:151030. doi:10.1155/2012/151030

5. Abzhanov A, Rodda SJ, McMahon AP, Tabin CJ. Regulation of skeletogenic differentiation in cranial dermal bone. *Development*. Sep 2007;134(17):3133-44. doi:10.1242/dev.002709

6. Wise GE, He H, Gutierrez DL, Ring S, Yao S. Requirement of alveolar bone formation for eruption of rat molars. *Eur J Oral Sci*. Oct 2011;119(5):333-8. doi:10.1111/j.1600-0722.2011.00854.x

7. Pieles O, Reck A, Morsczeck C. High endogenous expression of parathyroid hormone-related protein (PTHrP) supports osteogenic differentiation in human dental follicle cells. *Histochem Cell Biol*. Oct 2020;154(4):397-403. doi:10.1007/s00418-020-01904-7

8. Chen J, Lan Y, Baek JA, Gao Y, Jiang R. Wnt/beta-catenin signaling plays an essential role in activation of odontogenic mesenchyme during early tooth development. *Dev Biol*. Oct 2009;334(1):174-85. doi:10.1016/j.ydbio.2009.07.015

9. Chen J, Cheng J, Zhao C, Zhao B, Mi J, Li W. The Hippo pathway: a renewed insight in the craniofacial diseases and hard tissue remodeling. *Int J Biol Sci*. 2021;17(14):4060-4072. doi:10.7150/ijbs.63305

10. Pandya M, Gopinathan G, Tillberg C, Wang J, Luan X, Diekwisch TGH. The Hippo Pathway Effectors YAP/TAZ Are Essential for Mineralized Tissue Homeostasis in the Alveolar Bone/Periodontal Complex. *J Dev Biol*. Mar 01 2022;10(1)doi:10.3390/jdb10010014

11. Hathaway-Schrader JD, Novince CM. Maintaining homeostatic control of periodontal bone tissue. *Periodontol 2000*. Jun 2021;86(1):157-187. doi:10.1111/prd.12368

12. Ono W, Sakagami N, Nishimori S, Ono N, Kronenberg HM. Parathyroid hormone receptor signalling in osterix-expressing mesenchymal progenitors is essential for tooth root formation. *Nat Commun*. Apr 2016;7:11277. doi:10.1038/ncomms11277

13. Takahashi A, Nagata M, Gupta A, et al. Autocrine regulation of mesenchymal progenitor cell fates orchestrates tooth eruption. *Proc Natl Acad Sci U S A*. 01 2019;116(2):575-580. doi:10.1073/pnas.1810200115

14. Nagata M, Ono N, Ono W. Mesenchymal Progenitor Regulation of Tooth Eruption: A View from PTHrP. *J Dent Res*. Oct 2019:22034519882692. doi:10.1177/0022034519882692

15. de Crombrugghe B, Lefebvre V, Nakashima K. Regulatory mechanisms in the pathways of cartilage and bone formation. *Curr Opin Cell Biol*. Dec 2001;13(6):721-7. doi:10.1016/s0955-0674(00)00276-3

16. Bergwitz C, Jüppner H. Regulation of phosphate homeostasis by PTH, vitamin D, and FGF23. *Annu Rev Med*. 2010;61:91-104. doi:10.1146/annurev.med.051308.111339

17. Wein MN, Kronenberg HM. Regulation of Bone Remodeling by Parathyroid Hormone. *Cold Spring Harb Perspect Med*. Aug 01 2018;8(8)doi:10.1101/cshperspect.a031237

18. Proffit WR, Frazier-Bowers SA. Mechanism and control of tooth eruption: overview and clinical implications. *Orthod Craniofac Res*. May 2009;12(2):59-66. doi:10.1111/j.1601-6343.2009.01438.x

19. Frazier-Bowers SA, Simmons D, Wright JT, Proffit WR, Ackerman JL. Primary failure of eruption and PTH1R: the importance of a genetic diagnosis for orthodontic treatment planning.

Am J Orthod Dentofacial Orthop. Feb 2010;137(2):160.e1-7; discussion 160-1. doi:10.1016/j.ajodo.2009.10.019

20. Grippaudo C, Cafiero C, D'Apolito I, Ricci B, Frazier-Bowers SA. Primary failure of eruption: Clinical and genetic findings in the mixed dentition. *Angle Orthod*. May 2018;88(3):275-282. doi:10.2319/062717-430.1

21. Zhao Y, Zhang G. A computational study of the dual effect of intermittent and continuous administration of parathyroid hormone on bone remodeling. *Acta Biomater*. Jul 15 2019;93:200-209. doi:10.1016/j.actbio.2019.04.007

22. Zhang K, Zhang FJ, Zhao WJ, Xing GS, Bai X, Wang Y. Effects of parathyroid hormone-related protein on osteogenic and adipogenic differentiation of human mesenchymal stem cells. *Eur Rev Med Pharmacol Sci*. Jun 2014;18(11):1610-7.

23. Jilka RL, Weinstein RS, Bellido T, Roberson P, Parfitt AM, Manolagas SC. Increased bone formation by prevention of osteoblast apoptosis with parathyroid hormone. *J Clin Invest*. Aug 1999;104(4):439-46. doi:10.1172/JCI6610

24. Dobnig H, Turner RT. Evidence that intermittent treatment with parathyroid hormone increases bone formation in adult rats by activation of bone lining cells. *Endocrinology*. Aug 1995;136(8):3632-8. doi:10.1210/endo.136.8.7628403

25. Cheloha RW, Gellman SH, Vilardaga JP, Gardella TJ. PTH receptor-1 signalling-mechanistic insights and therapeutic prospects. *Nat Rev Endocrinol*. Dec 2015;11(12):712-24. doi:10.1038/nrendo.2015.139

26. Wein MN, Foretz M, Fisher DE, Xavier RJ, Kronenberg HM. Salt-Inducible Kinases: Physiology, Regulation by cAMP, and Therapeutic Potential. *Trends Endocrinol Metab*. 10 2018;29(10):723-735. doi:10.1016/j.tem.2018.08.004

27. Sakamoto K, Bultot L, Göransson O. The Salt-Inducible Kinases: Emerging Metabolic Regulators. *Trends Endocrinol Metab*. Dec 2018;29(12):827-840. doi:10.1016/j.tem.2018.09.007

28. Berdeaux R, Goebel N, Banaszynski L, et al. SIK1 is a class II HDAC kinase that promotes survival of skeletal myocytes. *Nat Med*. May 2007;13(5):597-603. doi:10.1038/nm1573

29. Wein MN, Liang Y, Goransson O, et al. SIKs control osteocyte responses to parathyroid hormone. *Nat Commun*. 10 2016;7:13176. doi:10.1038/ncomms13176

30. Wein MN, Spatz J, Nishimori S, et al. HDAC5 controls MEF2C-driven sclerostin expression in osteocytes. *J Bone Miner Res*. Mar 2015;30(3):400-11. doi:10.1002/jbmr.2381

31. Nishimori S, O'Meara MJ, Castro CD, et al. Salt-inducible kinases dictate parathyroid hormone 1 receptor action in bone development and remodeling. *J Clin Invest*. Dec 02 2019;129(12):5187-5203. doi:10.1172/JCI130126

32. Wang J, Martin JF. Hippo Pathway: An Emerging Regulator of Craniofacial and Dental Development. *J Dent Res*. Oct 2017;96(11):1229-1237. doi:10.1177/0022034517719886

33. Wang J, Liu S, Heallen T, Martin JF. The Hippo pathway in the heart: pivotal roles in development, disease, and regeneration. *Nat Rev Cardiol*. Nov 2018;15(11):672-684. doi:10.1038/s41569-018-0063-3

34. Cong Q, Liu Y, Zhou T, et al. A self-amplifying loop of YAP and SHH drives formation and expansion of heterotopic ossification. *Sci Transl Med*. Jun 23 2021;13(599)doi:10.1126/scitranslmed.abb2233

35. Nishioka N, Inoue K, Adachi K, et al. The Hippo signaling pathway components Lats and Yap pattern Tead4 activity to distinguish mouse trophectoderm from inner cell mass. *Dev Cell*. Mar 2009;16(3):398-410. doi:10.1016/j.devcel.2009.02.003

36. Xu T, Wang W, Zhang S, Stewart RA, Yu W. Identifying tumor suppressors in genetic mosaics: the Drosophila lats gene encodes a putative protein kinase. *Development*. Apr 1995;121(4):1053-63. doi:10.1242/dev.121.4.1053

37. McPherson JP, Tamblyn L, Elia A, et al. Lats2/Kpm is required for embryonic development, proliferation control and genomic integrity. *EMBO J*. Sep 15 2004;23(18):3677-88. doi:10.1038/sj.emboj.7600371

38. St John MA, Tao W, Fei X, et al. Mice deficient of Lats1 develop soft-tissue sarcomas, ovarian tumours and pituitary dysfunction. *Nat Genet*. Feb 1999;21(2):182-6. doi:10.1038/5965

39. Cruciat CM, Niehrs C. Secreted and transmembrane wnt inhibitors and activators. *Cold Spring Harb Perspect Biol*. Mar 01 2013;5(3):a015081. doi:10.1101/cshperspect.a015081

40. Liu J, Xiao Q, Xiao J, et al. Wnt/β-catenin signalling: function, biological mechanisms, and therapeutic opportunities. *Signal Transduct Target Ther*. Jan 03 2022;7(1):3. doi:10.1038/s41392-021-00762-6

41. Qiu W, Chen L, Kassem M. Activation of non-canonical Wnt/JNK pathway by Wnt3a is associated with differentiation fate determination of human bone marrow stromal (mesenchymal) stem cells. *Biochem Biophys Res Commun*. Sep 16 2011;413(1):98-104. doi:10.1016/j.bbrc.2011.08.061

42. Miyabara S, Yuda Y, Kasashima Y, Kuwano A, Arai K. Regulation of Tenomodulin Expression Via Wnt/β-catenin Signaling in Equine Bone Marrow-derived Mesenchymal Stem Cells. *J Equine Sci*. 2014;25(1):7-13. doi:10.1294/jes.25.7

43. Logan CY, Nusse R. The Wnt signaling pathway in development and disease. *Annu Rev Cell Dev Biol*. 2004;20:781-810. doi:10.1146/annurev.cellbio.20.010403.113126

44. Rahman MS, Akhtar N, Jamil HM, Banik RS, Asaduzzaman SM. TGF-β/BMP signaling and other molecular events: regulation of osteoblastogenesis and bone formation. *Bone Res*. 2015;3:15005. doi:10.1038/boneres.2015.5

45. Goes P, Dutra C, Lösser L, Hofbauer LC, Rauner M, Thiele S. Loss of Dkk-1 in Osteocytes Mitigates Alveolar Bone Loss in Mice With Periodontitis. *Front Immunol*. 2019;10:2924. doi:10.3389/fimmu.2019.02924

46. Yao Y, Kauffmann F, Maekawa S, et al. Sclerostin antibody stimulates periodontal regeneration in large alveolar bone defects. *Sci Rep*. Oct 01 2020;10(1):16217. doi:10.1038/s41598-020-73026-y

47. Tang CC, Castro Andrade CD, O'Meara MJ, et al. Dual targeting of salt inducible kinases and CSF1R uncouples bone formation and bone resorption. *Elife*. Jun 23 2021;10doi:10.7554/eLife.67772

48. Zhang J, Liao L, Li Y, et al. Parathyroid hormone-related peptide (1-34) promotes tooth eruption and inhibits osteogenesis of dental follicle cells during tooth development. *J Cell Physiol*. Jul 2019;234(7):11900-11911. doi:10.1002/jcp.27857

49. Ruzankina Y, Pinzon-Guzman C, Asare A, et al. Deletion of the developmentally essential gene ATR in adult mice leads to age-related phenotypes and stem cell loss. *Cell Stem Cell*. Jun 07 2007;1(1):113-26. doi:10.1016/j.stem.2007.03.002

50. Bouxsein ML, Boyd SK, Christiansen BA, Guldberg RE, Jepsen KJ, Müller R. Guidelines for assessment of bone microstructure in rodents using micro-computed tomography. *J Bone Miner Res*. Jul 2010;25(7):1468-86. doi:10.1002/jbmr.141

51. Yoon SH, Meyer MB, Arevalo C, et al. A parathyroid hormone/salt-inducible kinase signaling axis controls renal vitamin D activation and organismal calcium homeostasis. *J Clin Invest*. May 01 2023;133(9)doi:10.1172/JCI163627

52. Sasagawa S, Takemori H, Uebi T, et al. SIK3 is essential for chondrocyte hypertrophy during skeletal development in mice. *Development*. Mar 2012;139(6):1153-63. doi:10.1242/dev.072652

53. Norris RA, Damon B, Mironov V, et al. Periostin regulates collagen fibrillogenesis and the biomechanical properties of connective tissues. *J Cell Biochem*. Jun 01 2007;101(3):695-711. doi:10.1002/jcb.21224

54. Padbury AD, Tözüm TF, Taba M, et al. The impact of primary hyperparathyroidism on the oral cavity. *J Clin Endocrinol Metab*. Sep 2006;91(9):3439-45. doi:10.1210/jc.2005-2282

55. Chan HL, McCauley LK. Parathyroid hormone applications in the craniofacial skeleton. *J Dent Res*. Jan 2013;92(1):18-25. doi:10.1177/0022034512464779

56. Shen L, He Y, Chen S, He L, Zhang Y. PTHrP Modulates the Proliferation and Osteogenic Differentiation of Craniofacial Fibrous Dysplasia-Derived BMSCs. *Int J Mol Sci*. Apr 20 2023;24(8)doi:10.3390/ijms24087616

57. Fraser WD, Walsh CA, Birch MA, et al. Parathyroid hormone-related protein in the aetiology of fibrous dysplasia of bone in the McCune Albright syndrome. *Clin Endocrinol (Oxf)*. Nov 2000;53(5):621-8. doi:10.1046/j.1365-2265.2000.01112.x

58. Maes C, Kronenberg HM. Chapter 60 - Bone Development and Remodeling. In: Jameson JL, De Groot LJ, de Kretser DM, et al, eds. *Endocrinology: Adult and Pediatric (Seventh Edition)*. W.B. Saunders; 2016:1038-1062.e8.